

Time series analysis for medical videos

Henrik Løland Gjestang



Thesis submitted for the degree of
Master in Computational Science
(Imaging and Biomedical Computing)
60 credits

Department of Informatics
Faculty of mathematics and natural sciences

UNIVERSITY OF OSLO

Spring 2020

Time series analysis for medical videos

Henrik Løland Gjestang

© 2020 Henrik Løland Gjestang

Time series analysis for medical videos

<http://www.duo.uio.no/>

Printed: Reprosentralen, University of Oslo

Abstract

This is the abstract part. How does it look? This is the abstract part. How does it look? This is the abstract part. How does it look? This is the abstract part. How does it look?

Acknowledgements

This thesis is submitted as part of the master's degree in informatics: Computational Science: Imaging and Biomedical Computing. It has been very interesting to work with ..

I would especially like to thank my supervisor Pål for ..

Thanks to my internal supervisor Professor Anne H. Solberg and the rest of the DSB group, for....

Finally, I would like to thank my parents for their encouragement and everlasting love.

Contents

List of Figures	vi
List of Tables	vii
List of Symbols	viii
1 Introduction	1
1.1 Background and Motivation	1
1.2 Problem statement	1
1.3 Scope and limitations	2
1.4 Research methods	2
1.5 Main Contributions	2
1.6 Thesis Outline	2
2 Background	3
2.1 Medical scenario	3
2.1.1 Colon cancer	3
2.1.2 The digestive system	3
2.1.3 Traditional Endoscopy	3
2.1.4 Wireless Capsule Endoscopy	3
2.2 Artificial intelligence and Machine learning	4
2.2.1 Imbalanced data	6
2.2.2 TensorFlow	6
2.2.3 Data pipeline	6
2.2.4 How to evaluate a model	6
2.2.5 Convolutional Neural Network	6
2.3 Related work	8
2.3.1 Object tracking	9
2.3.2 Segmentation	9
2.3.3 Mapping	10
2.4 Summary	10
3 Methodology	11
3.1 Data collection	11
3.1.1 Kvasir PillCam	11
3.1.2 Kvasir	12
3.1.3 Hyper Kvasir	12
3.2 Data process	13
3.2.1 Data preprocessing	13
3.2.2 Data pipeline	13
3.3 System implementation	13
3.4 Summary	13
4 Experiments	14
4.1 Results	14
4.2 Summary	14

5 Conclusions **15**
 5.1 Summary and contributions 15
 5.2 Future work 15
Bibliography **16**

List of Figures

1.1	Illustration of how such a camera pill could look like	1
2.1	An overview of the terms used to describe the digestive system	4
2.2	Image of a fiber optic endoscope with explanation of different parts of the tool . .	5
2.3	Images taken with WCE	5
2.4	Illustration of how object in two frames is tracked with a bounding box	9
2.5	An example of Deep EndoVO accuracy	10
3.1	Example of a segmented image from Hyper-Kvasir dataset.	12

List of Tables

2.1	Segmentation results on the ISBI cell tracking challenge in 2015	10
3.1	PillCam class names and corresponding class numbers.	11
3.2	Kvasir class names and corresponding class numbers.	12

List of Symbols

x position

Chapter 1

Introduction

1.1 Background and Motivation

In this project we aim to design and develop a system for analyzing medical videos from a camera pill, as seen in Figure 1.1. The pill is swallowed and records video of the entire digestive system. The goal is to be able to detect different irregularities in the patients digestive system, like a colon polyp, Chron's disease, Colorectal cancer, etc. by using video object tracking, object detection, machine learning or other relevant tools.

Neural networks models that we would like to explore further for this purpose are Convolutional neural networks (CNN), Recurrent neural networks (RNN), Capsule neural networks, Long Short-Term memory networks and more.

The main idea is to go beyond image-based methods and also exploit the time factor of the data. The videos we will be using for this is delivered by Bærum Hospital, and is carefully labeled by using tools such as described in the paper “Expert Driven Semi-Supervised Elucidation Tool for Medical Endoscopic Videos”. In this paper Albisser *et al.* presents a semi-supervised method to gather the annotations in a easy and time saving way [1].



Figure 1.1: Illustration of how such a camera pill could look like [2].

1.2 Problem statement

Colorectal cancer (CRC) is the third most common cause of cancer mortality for both men and women [3], and it is a condition where early detection is of clear value for the ultimate survival of the patient. As statistics show that 15% of male and female above 50 years are at risk, the

procedure is recommended on a regular basis (every 3-5 years) for the population over 50, and from an earlier age for high-risk groups.

Colonoscopy is a demanding procedure requiring an significant amount of time by specialized physicians, in addition to the discomfort and risks inherent in the procedure. Traditional methods based on colonoscopy are not cost-effective for population-based screening purposes, so only about 2-3% of the target population is reached at present.

The cost of a population screening program is prohibitively expensive. Colonoscopy is the most expensive cancer screening process in the US, with annual costs of \$10 billion dollars (\$1100 per person). In Norway we have similar costs of around \$1000 per person, with a time consumption of about 1 doctor-hour and 2 nurse-hours per examination.

By researching an automatic system for a camera pill the aim is to greatly increase the number of patients that can be examined, i.e., making the public health care system more scalable and cost effective, while at the same time reducing the need for intrusive procedures like "bottom-up" examinations like colonoscopy.

1.3 Scope and limitations

Based on the described problem statement the scope of this thesis is to compare some prior selected automatic systems, with a focus on machine learning, for classification tasks in the medical domain. We will test the systems on video and still images taken from a wireless capsule endoscopy system, provided by Bærum Hospital. This data is generated with PillCamTM SB 3 System¹ and gives us a wide view of the GI-tract. A limitation for our research will therefore be that our dataset lack a great deal of diversity. While we might have a wide range of 'patient' all the data contributions stem from one provider in one location. This might not be much of an issue due to GI-tract being quite homogenous over large populations.

By using a tool provided by Augere Medical, we have sequentially classified each frame in some 45 PillCam videos. Although being assisted by doctor Thomas de Lange, with many years of experience, the dataset might not be perfectly labeled due to time constraints. But to the best of our efforts we managed to divide the data into 10 classes which we later will train our networks on.

Considering the scope of this thesis, we will limit ourselves to use some of the more common deep convolutional neural networks and a more novel stacked hourglass network. There are many other more common network used in the field of object classification like NN, RNN, stastistical methods, but these methods are widely tested and we wish to push the envelope of machine learning systems on medical videos and also have a wide variety of ways to score our model against previously tested algorithms.

1.4 Research methods

Reference symbols: x

1.5 Main Contributions

1.6 Thesis Outline

¹<https://www.medtronic.com/covidien/en-us/products/capsule-endoscopy/pillcam-sb-3-system.html>

Chapter 2

Background

2.1 Medical scenario

2.1.1 Colon cancer

2.1.2 The digestive system

To detect irregularities in the digestive system (Figure 2.1) is a difficult and time-consuming task. To classify irregularities correctly and precisely require expert knowledge. Fortunately we have access to data which already has been labeled by trained professionals that we will use in this project.

The most common way of screening patients is with a endoscope. When this tool is used by a professional some of the irregularities that can be spotted are; *Colon polyp*, *Colorectal Cancer*, *Ulcerative Colitis*, *Crohn's Disease*, *Familial adenomatous polyposis*, *Diverticulosis* and *Diverticula Bleeding*.

These diseases have varying patterns and while some can be easy to split apart, some are more similar in pattern. While for an untrained eye it can be easy to spot that something is wrong it is very difficult to describe with words what that might be or even harder to write a program to detect the correct characteristic features of the disease. This is why we rely on having good amount of labeled data for this project to work. For increased accuracy we may have to look closer at a couple of diseases. Preferably two irregularities that both have different characteristics and lots of labeled training data.

2.1.3 Traditional Endoscopy

2.1.4 Wireless Capsule Endoscopy

The basic technology behind the modern endoscope was developed in the early 1950s by English physicist Harold Hopkins and his student Narinder Kapany which let light travel through flexible pieces of glass, now known as optical fibers [4].

Before the year 2000 the only option you had to visualize the food pipe, stomach, duodenum, colon and terminal ileum (see Figure 2.1 for details) was to use a fiber-optic endoscope, which is a tool with a relatively wide cable that is pushed into the bowel with as much as 50 000 optic fibers (as seen on Figure 2.2). These cables have to carry fiber optic bundles, water pipes, operations channel and control cables. Although these cables can be quite flexible there is a limit for how far they can advance into the small bowel. This method cause pain and discomfort for the patient, and there was a clinical need for an improved methods.

That is why in the year 2000 Iddan *et al.* developed a new type of video-telemetry capsule endoscope that was swallowable [5]. It could travel through the entire digestive system because it had no external wires, fiber-optic bundles or cables of any sort. The capsule travels by peristalsis³ through the gastrointestinal tract, which takes from 10 to 48 hours, and transmit images on a

¹ By Mariana Ruiz, edited by Joaquim Gaspar. Released into public domain by author.
https://en.wikipedia.org/wiki/File:Digestive_system_diagram_edit.svg

² Image credit: Jacaranda Physics 1 2nd Edition © John Wiley & Sons, Inc.

³Peristalsis is a radially symmetrical contraction and relaxation of muscles that propagates in a wave down a tube, in an antegrade direction.

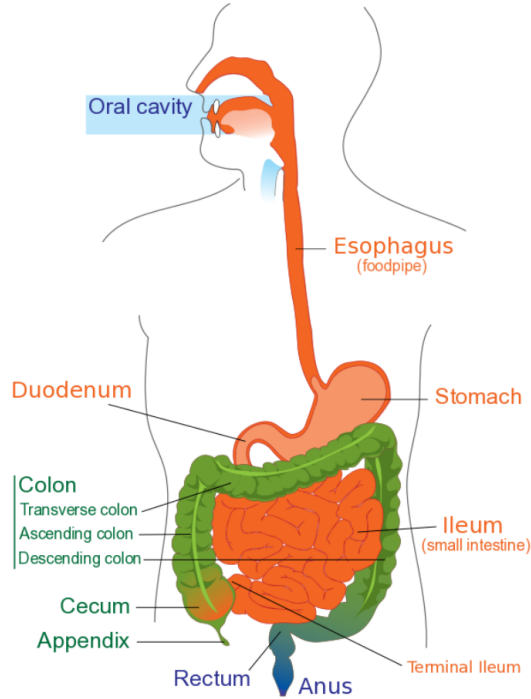


Figure 2.1: An overview of the terms used to describe the digestive system¹.

regular interval to receivers attached around the outside of the patients stomach for as long as the battery allows, usually in the range 6 to 8 hours. Two example images taken by WCE are presented in Figure 2.3. By triangulating the signal strength and the location of the receivers taped on the body it is possible to roughly estimate the position of the capsule. This is however not very precise and can not tell us the rotation or direction of the capsule. Regardless, that information will not be available for us in this study as we only have access to the images themselves. Therefore we could implement an algorithm to predict which region of the digestive system the image is taken from (see section 2.3.3).

2.2 Artificial intelligence and Machine learning

As apposed to using regular optic-fiber endoscopy, it can be difficult to know the location and orientation of the capsule when it is traveling through the digestive system. In a paper by Zou *et al.* it is shown that by using Deep Convolutional Networks (DCNN) it is possible to classify the digestive organs in wireless capsule endoscopy with about 95% classification accuracy on average [6]. The DCNN-based WCE digestive organ classification system is constructed of three stages of convolution, pooling and two fully-connected layers. This is illustrated in Figure 3 in the paper [6]. The main steps of this convolutional neural network are described in detail in section 2.2.5.

⁴ CC BY-SA 3.0 / Attribution to Dr.HH.Krause at English Wikipedia;
https://commons.wikimedia.org/wiki/File:Normales_Colon.PNG
<https://commons.wikimedia.org/wiki/File:Dunndarm.PNG>

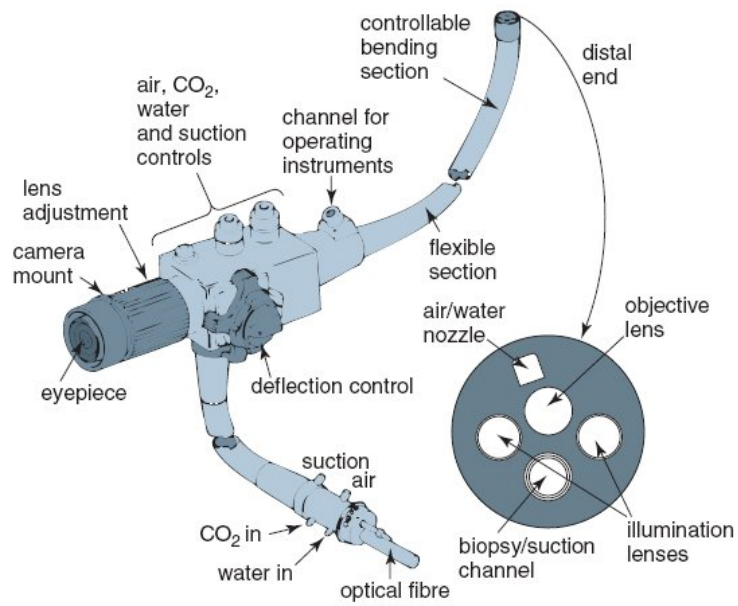


Figure 2.2: Image of a fiber optic endoscope with explanation of different parts of the tool².



(a) Small Intestine



(b) Colon

Figure 2.3: Images taken with WCE⁴.

2.2.1 Imbalanced data

2.2.2 TensorFlow

2.2.3 Data pipeline

2.2.4 How to evaluate a model

2.2.5 Convolutional Neural Network

One of the most used neural networks for image classification is the Convolutional Neural Network (CNN). The model was first proposed by Krizhevsky *et al.* in 2012 [7] where they trained a deep convolutional neural network and used it to classify 1.2 million high-resolution images in the ImageNet LSVRC-2010 contest into the 1000 different classes with top-1 and top-5 error rates of 37.5% and 17.0% which far surpassed all other models at the time. Next we will get into a bit of the details of a CNN.

Convolution layer

The first step in a convolutional neural network is to extract features from the input image. This is done to preserve the relationship between pixels by learning image features using filters, or *kernels*. As a result, the network learn filters that activate when it detects some specific patterns or features.

The convolution of f and g is written as $f * g$, and is defined as the integral of the product of the two functions after one (usually the filter) is reversed and shifted.

$$(f * g)(t) = \int_{-\infty}^{\infty} f(\tau)g(t - \tau)d\tau \quad (2.1)$$

Non Linearity (ReLU)

Rectified Linear unit function, known as simply ReLU, is an activation function represented by equation (2.2). It sets all negative numbers to zero, by discarding them from the activation map entirely. In this way, ReLU increases the nonlinear properties of the decision function and thus of the overall network without affecting the receptive fields of the convolution layer.

$$ReLU(x) = \max(0, x) \quad (2.2)$$

Pooling layer

Pooling layers are applied to reduce the number of parameters when the images are considerably large. Spatial pooling, or merely down sampling, reduces the dimensionality of each image but it keeps the important information. The most used down sampling is max pooling. It extracts the largest element from the rectified feature map and thus reduces computational complexity of the algorithm. In addition average pooling is also frequently used, this method computes the average value of the input map. The input-output model is denoted as:

$$y_i = f(\text{pool}(x_i)) \quad (2.3)$$

Fully-connected layer

In a FC-layer every neuron in one layer is connected to every neuron in the previous layer. It is here the high-level reasoning is done. The activation function in the neurons is a *sigmoid* or *tanh* function.

$$f(z) = \frac{1}{1 + \exp(-z)} \quad \text{or} \quad f(z) = \tanh(z) = \frac{e^z - e^{-z}}{e^z + e^{-z}} \quad (2.4)$$

At the end of FC-layer we have an activation function such as softmax (equation 2.7) to calculate probability of the predicted classes.

Feed Forward

In the feed forward algorithm input image will be processed through all the layers in the neural network. The first layer will be a convolution layer, containing K filters F_i^1 , $i = 1, \dots, K$, of size $k \times k$ and a bias b^1 . The image will be convoluted with each filter, and the bias is added.

$$\hat{z}_i^l = I * \hat{F}_i^l + b^l, \quad (2.5)$$

where $*$ (asterisk) is the convolution operator in equation 2.1. The final output of each convolutional layer l is a^l ,

$$\hat{a}_i^l = f(z_i^l), \quad (2.6)$$

where f represents the ReLU activation function. After going through the convolution layer, the next layer could be a pooling layer, which will reduce the spatial dimensionality either by using the max value or the average value. Before getting our final output \hat{y} , we need to collect the outputs from all the filters, which will be an input to a fully connected layer. The fully connected layer use the softmax activation function to classify the input image, much like a neural network would. The softmax function is an accepted standard probability function for a multiclass classifier [8]. The total sum of the probabilities will always add up to 1 when using softmax.

$$\sigma(z)_j = \frac{e^{z_j}}{\sum_{k=1}^K e^{z_k}} \quad \text{for } j = 1, \dots, K. \quad (2.7)$$

To calculate the error of the forward propagation it is common to use cross-entropy error function.

$$C(\hat{y}) = - \sum_{i=1}^N t_i \log(y_i) \quad (2.8)$$

Back propagation

Starting from the last layer L , we calculate the derivative of the loss function (function 2.8) with regards to the activation function in order to update the weights. Computing the gradient of the loss function yields

$$\frac{\partial C}{\partial y_i} = -\frac{t_i}{y_i} \quad (2.9)$$

We also require the gradient of the output of the final layer y_i with regards to the input z_k^L of the activation function (equation 2.7)

$$\frac{\partial y_i}{\partial z_k^L} = \begin{cases} y_i(1 - y_i), & i = k \\ -y_i y_k, & i \neq k \end{cases} \quad (2.10)$$

Now with regards to z_i^L

$$\begin{aligned} \frac{\partial C}{\partial z_i^L} &= \sum_k^N \frac{\partial C}{\partial y_k} \frac{\partial y_k}{\partial z_i^L} \\ &= \frac{\partial C}{\partial y_i} \frac{\partial y_i}{\partial z_i^L} - \sum_k^N \frac{\partial C}{\partial y_k} \frac{\partial y_k}{\partial z_i^L} \\ &= -t_i(1 - y_i) + \sum_{k \neq i} t_k y_i \\ &= y_i - t_i \end{aligned} \quad (2.11)$$

And finally with regards to the weights

$$\frac{\partial C}{\partial w_{ij}^L} = (y_i - t_i) a_j^{L-1} \quad (2.12)$$

where \hat{a}_j^{L-1} is the vectorized output from the previous layer. From here, we will propagate the error throughout the layers. The error with regards to the input a_i^L to the fully connected layer is:

$$\delta^{L-1} = \frac{\partial C}{\partial a_i^L} = \sum_i^N (y_i - t_i) w_{ji}^L \quad (2.13)$$

Thus the error is propagated backwards through each layer. If max pooling was used in a pooling layer, the error will only be propagated to the input that had the highest value in the forward pass. The other values will be set to zero. If average pooling was used, the error is averaged in the backwards pass. In equation 2.13 a^l is the output of a convolutional layer l . Since a convolutional layer is always preceded and followed by a activation layer, the input to layer l is $a^{l-1} = \sigma(z^l)$. Now consider the error with regards to z^l .

$$\begin{aligned} \delta_{ij}^l &= \frac{\partial C}{\partial z_{ij}^l} \\ &= \sum_{i'}^I \sum_{j'}^I \frac{\partial C}{\partial z_{i'j'}^{l+1}} \frac{\partial z_{i'j'}^{l+1}}{\partial z_{ij}^l} \\ &= \sum_{i'}^I \sum_{j'}^I \delta_{i'j'}^{l+1} \frac{\partial (\hat{W}\sigma(z^l) + b^{l+1})}{\partial z_{ij}^l} \\ &= \delta^{l+1} * ROT180(w^{l+1})\sigma'(z^l) \end{aligned} \quad (2.14)$$

Having found the error, the gradient of the cost function with regards to the weights is

$$\frac{\partial C}{\partial w_{ij}^l} = \delta_{ij}^l * \sigma ROT180(z_{ij}^{l-1}) \quad (2.15)$$

2.3 Related work

Zhu *et al.* have made a computer-aided lesion⁵ detection system which uses a trainable feature extractor, also based on a CNN, and feed the generic features to a Support Vector Machine which enhance the generalization ability [9]. This method greatly outperform the earlier methods based on color and texture features. However we believe that by using neural networks to do the decision making we can further improve this detection system.

Yuan *et al.* have accomplished an average overall recognition accuracy of 98.0% for detecting polyps in WCE images by using a deep feature learning method, named stacked sparse autoencoder with image manifold constraint (SSAEIM). This method is built on a Sparse auto-encoder (SAE), a symmetrical and unsupervised neural network. It is an encoder-decoder architecture where the encoder network encodes pixel intensities as low dimensional attributes, while the decoder step reconstructs the original pixel intensities from the learned low-dimensional features [10]. Detecting colorectal polyps are important because they are precursors to cancer, which may develop if the polyps are left untreated. Where we hopefully can build on this method is by using a larger dataset with pathology proof of other irregularities.

Jia *et al.* present a new automatic bleeding detection strategy based on a deep convolutional neural network and evaluate their method on an expanded dataset of 10,000 WCE images. Gastrointestinal (GI) tract bleeding is the most common abnormality in the tract, but also an important symptom or syndrome of other pathologies such as ulcers, polyps, tumors and Crohn's disease. Their method for detecting bleeding have an increase of around 2 percentage in F_1 score, up to 0.9955 [11]. This method and its high score is somewhat limited to bleeding, and not very good at detecting other lesion. Our goal is to develop a method for using deep learning to find more generalized pathologies in the gastrointestinal tract.

We will go through some other methods not directly related to neural networks but which we think may come in handy for my thesis later on.

⁵a region in an organ or tissue which has suffered damage through injury or disease, such as a wound, ulcer, abscess, or tumor.

2.3.1 Object tracking

Object tracking is one of the harder problem to overcome in computer vision and is key to achieving good results in endoscopic video analysis. Tracking algorithms are developed to determine the movement of the object or objects in each video frame. The algorithm has to take into account the dynamic environment such as differences in lightning, occlusions and scaling changes. Also the absence of any prior knowledge to the object and its position further increase the complexity of the problem. Zhang *et al.* proposed an approach for visual tracking in videos that learns to predict the bounding box locations of a target object at every frame in the paper “Deep Reinforcement Learning for Visual Object Tracking in Videos” [12]. While other models depends on the capability of a CNN to learn a good feature representation for the target location in the new frame, which means that the model only tracks properly if the target lies in the spatial vicinity of the previous prediction. This is not always the case for WCE videos, where the lens of the camera can suddenly and unpredictably rotate towards the wall of the intestine. This method integrates convolutional network with recurrent network, and builds up a spatial-temporal representation of the video which means that the model is able to predict the target object’s location over time.

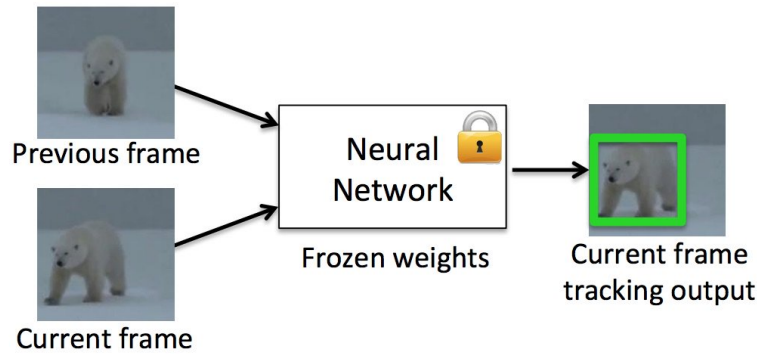


Figure 2.4: Illustration of how object in two frames is tracked with a bounding box⁶.

Our hope is that by implementing an object-tracking algorithm we can use it to classify irregularities in the colonoscopy video, and then track that object in the later frames until it disappear out of frame. This will hopefully help with reducing the robustness of the network so that the classifier will not have to check every frame for irregularities.

2.3.2 Segmentation

Image segmentation is the process of partitioning a image into multiple segments of pixel, usually each segment describing some feature of the image or an entire object or class of objects. The goal of segmentation is to simplify the image and make it easier to analyze or further process. Ronneberger *et al.* propose a method in the paper “U-Net: Convolutional Networks for Biomedical Image Segmentation” [13] for using a network and training strategy that relies on the strong use of data augmentation to use the available labeled samples more efficiently. This network outperform the old method of sliding-window-convolution by a great deal. They extend the “fully convolutional network” [14] such that it works with very few training images and yields more precise segmentations. The way this is achieved is to supplement a contracting network by successive layers, where instead of using pooling operators, upsampling operators are used. This means that these successive layers increase the resolution of the output. The high resolution features from the contracting path are combined with the upsampled output to localize objects and with that a convolution layer can then learn to produce more precise output based on this information.

Another important feature in this architecture is that in the upsampling portion of the network there is also large number of feature channels. These channels allow the network to pass on context information to the higher resolution layers.

A common problem in training neural networks are too little labeled training data. This is also the case for us. We require a lot of medical data, and personell with the expertise to correctly label

⁶ <https://www.learnopencv.com/goturn-deep-learning-based-object-tracking/>

Name	PhC-U373	DIC-HeLa
IMCB-SG (2014)	0.2669	0.2935
KTH-SE (2014)	0.7953	0.4607
HOUS-US (2014)	0.5323	-
second-best 2015	0.83	0.46
u-net (2015)	0.9203	0.7756

Table 2.1: Segmentation results on the ISBI cell tracking challenge in 2015.

our data are of high demand and they usually have very little time for projects like these. This is why Ronneberger *et al.* use different methods of data augmentation to generate more training data. They apply elastic deformations to the available images, and this allows the network to learn invariance to such deformations without the need to see these transformations in the annotated image corpus. Which is particular important in biomedical segmentation since deformation used to be the most common variation in tissue and realistic deformations can be simulated efficiently [13]. By doing this Ronneberger *et al.* were able to achieve very good results (Table 2.1).

2.3.3 Mapping

As mentioned in section 2.1.4, a concern when processing the images taken with a WCE is not having the spatial data you get when using a normal fiber-optic endoscope. This is why Turan *et al.* has recently made substantial progress in converting passive capsule endoscopes to active capsule robots, enabling more accurate, precise, and intuitive detection of the location and size of the diseased areas by developing reliable real time pose estimation functionality of the capsule with RCNN’s⁷ [15]. See Figure 2.5 for an example.

This architecture uses inception modules for feature extraction and a RNN for sequential modelling of motion dynamics to regress the robot’s orientation and position in real time. By taking multiple of RGB Depth images with timestamps it can calculate the 6-DoF pose of the capsule without the need of any extra sensors. For obtaining the depth images Turan *et al.* use the shape from shading (SfS) technique of Ping-Sing and Shah [16]. This model outperforms state-of-the-art models like LSD SLAM and ORB SLAM.

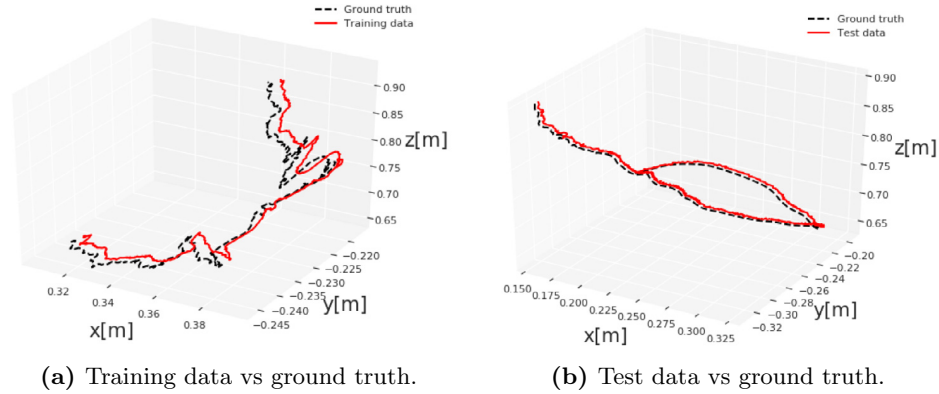


Figure 2.5: An example of Deep EndoVO accuracy [15].

2.4 Summary

⁷Deep recurrent convolutional neural networks

Chapter 3

Methodology

3.1 Data collection

The datasets used in our experiments are Kvasir Pillcam, Kvasir and Hyper-Kvasir. This section will demonstrate the main differences between the three datasets and explain how they can be found and used for fact checking. All three datasets are collected using endoscopic equipment at Vestre Viken Health Trust in Norway. The VV consists of 4 hospitals and provides health care for 470.000 people. One of the hospitals is Bærum Hospital, which has a large gastroenterology department from where the data is collected.

3.1.1 Kvasir PillCam

The dataset we used in our experiments consist of endoscopic videos collected from Bærum Hospital. Unlike Kvasir and Hyper-Kvasir datasets we have made the Kvasir PillCam dataset for the purpose of this thesis. In total we have 44 videos which have gone through some re encoding to reduce the file sizes, and also because the original encoding is proprietary Sony technology. After that the videos are uploaded to Augere Medical ¹ tagging tool. The data export from Bærum also contains some findings for each video (if there is any) and are extracted, converted to frame number and that helped us a great deal with tagging the videos. We also have Thomas de Lange to thank, because he helped us a lot with the medical aspect of the classification process. When all 44 videos have been precisely labeled the dataset is exported from Augeres tagging tool and split into folders for each class. The folders/classes are given in table 3.1. In total we have 44 000 labeled images in 8 classes. The sample distribution across the eight classes is skewed depending on how many findings there are in the videos. Some findings occur often and some very rarely. The dataset also contain one class for 'normal' images, which there is quite a bit more of than findings.

Imbalanced dataset pose a challenge for predictive algorithms as most learning algorithms are based on the assumption of an equal number of samples for each class. This results in models that have poor predictive performance, especially for minority class or classes. This is a great problem because in many medical datasets the minority class is the most important and therefore more sensitive for classification errors.

In addition to labeling the images the dataset also contain a JSON format file which stores coordinates for where in the frame the finding is located. The Kvasir Pillcam dataset will be an open-source dataset available for others scientists, and will later be grown to include more PillCam videos, both labeled and unlabeled samples.

¹<https://augere.md/>

Class number	Class name
0	normal
1	polyp
2	polyrus

Table 3.1: PillCam class names and corresponding class numbers.

Class number	Class name	Number of samples
0	normal	8000
1	polyp	8000
2	polypus	8000

Table 3.2: Kvasir class names and corresponding class numbers.

3.1.2 Kvasir

The Kvasir dataset [17] contains images from inside the gastrointestinal (GI) tract. The samples are classified into three important anatomical landmarks and three clinically significant findings. In addition it has two classes related to the removal procedure of polyps. The dataset is sorted and annotated is performed by medical doctors. The class names and findings for each class is given in table 3.2. One of the most important aspects of the Kvasir dataset is that it makes it easy to reproduce and compare results in scientific computing.

3.1.3 Hyper Kvasir

The Hyper-Kvasir dataset [18] is one of the largest medical datasets containing 110.079 images and 373 videos where it captures anatomical landmarks and pathological and normal findings. Resulting in more than 1.1 million images and video frames all together. The dataset contain four parts, labeled images, unlabeled images, segmented images and lastly, videos. In total the dataset is 70 GB in size, but can be downloaded and stored in parts from <https://datasets.simula.no/hyper-kvasir/>.

Labeled images

Hyper-Kvasir contains 10.662 labeled images. The images are split into 23 different classes, and are stored in a folder with the same name as its corresponding class. All of the images are stored in JPEG format [19], which means it has some image quality loss but quite insignificant compared to the reduction in file size. Like in situations most often encountered the classes has a different number of samples, this is a challenge in the medical field because some findings occur more often than others.

Unlabeled images

This part of the dataset contains 99.417 images

segmented images

In figure 3.1 we can see an example of the segmented Kvasir images.



Figure 3.1: Example of a segmented image from Hyper-Kvasir dataset.

Videos

3.2 Data process

3.2.1 Data preprocessing

3.2.2 Data pipeline

3.3 System implementation

3.4 Summary

Chapter 4

Experiments

4.1 Results

4.2 Summary

Chapter 5

Conclusions

5.1 Summary and contributions

We have looked on some highly relevant papers written about automatic detection systems for medical videos from the last few years. From back when feature extraction methods consisted of selecting color and intensities thresholds, to newer and more sophisticated algorithms like CNN's have become mainstream. The newer methods may be more complex and harder to implement but we have found that these automatic feature extraction methods have a far higher accuracy and produce less false positives. We have also looked at the importance of having a big and varied dataset with labeled data. If the dataset is not large enough we can use several data augmentation methods to increase it, like the ones used in U-Net.

5.2 Future work

Bibliography

- [1] Z. Albisser, M. Riegler, P. Halvorsen, J. Zhou, C. Griwodz, I. Balasingham, and C. Gurrin, “Expert driven semi-supervised elucidation tool for medical endoscopic videos”, in *Proceedings of the 6th ACM Multimedia Systems Conference*, 2015, pp. 73–76 (cit. on p. 1).
- [2] *PillCam - A Camera Pill System for Automatic Screening of the Digestive System - Institutt for informatikk*.
<https://www.mn.uio.no/ifi/studier/masteroppgaver/nd/SRL-media-pill-cam.html> (cit. on p. 1).
- [3] A. Jemal, R. Siegel, J. Xu, and E. Ward, “Cancer Statistics”, *CA: A Cancer Journal for Clinicians*, vol. 60, no. 5, pp. 277–300, 2010 (cit. on p. 1).
- [4] A. C. S. Van Heel, “A New Method of transporting Optical Images without Aberrations”, *Nature*, vol. 173, no. 4392, pp. 39–39, Jan. 1954 (cit. on p. 3).
- [5] G. Iddan, G. Meron, A. Glukhovsky, and P. Swain, “Wireless capsule endoscopy”, *Nature*, vol. 405, no. 6785, p. 417, May 2000 (cit. on p. 3).
- [6] Y. Zou, L. Li, Y. Wang, J. Yu, Y. Li, and W. J. Deng, “Classifying digestive organs in wireless capsule endoscopy images based on deep convolutional neural network”, in *Proceedings of the 2015 IEEE International Conference on Digital Signal Processing (DSP)*, Jul. 2015, pp. 1274–1278 (cit. on p. 4).
- [7] A. Krizhevsky, I. Sutskever, and G. E. Hinton, “ImageNet Classification with Deep Convolutional Neural Networks”, in *Advances in Neural Information Processing Systems 25*, 2012, pp. 1097–1105 (cit. on p. 6).
- [8] P. Sadowski, “Notes on backpropagation”, 2016 (cit. on p. 7).
- [9] R. Zhu, R. Zhang, and D. Xue, “Lesion detection of endoscopy images based on convolutional neural network features”, in *Proceedings of the 2015 8th International Congress on Image and Signal Processing (CISP)*, Oct. 2015, pp. 372–376 (cit. on p. 8).
- [10] Y. Yuan and M. Q.-H. Meng, “Deep learning for polyp recognition in wireless capsule endoscopy images”, *Medical Physics*, vol. 44, no. 4, pp. 1379–1389, Apr. 2017 (cit. on p. 8).
- [11] X. Jia and M. Q.-. Meng, “A deep convolutional neural network for bleeding detection in Wireless Capsule Endoscopy images”, in *Proceedings of the 2016 38th Annual International Conference of the IEEE Engineering in Medicine and Biology Society (EMBC)*, Aug. 2016, pp. 639–642 (cit. on p. 8).
- [12] D. Zhang, H. Maei, X. Wang, and Y.-F. Wang, “Deep Reinforcement Learning for Visual Object Tracking in Videos”, *arXiv:1701.08936 [cs]*, Jan. 2017. arXiv: 1701.08936 [cs] (cit. on p. 9).
- [13] O. Ronneberger, P. Fischer, and T. Brox, “U-Net: Convolutional Networks for Biomedical Image Segmentation”, in *Proceedings of the Medical Image Computing and Computer-Assisted Intervention*, 2015, pp. 234–241 (cit. on pp. 9, 10).
- [14] J. Long, E. Shelhamer, and T. Darrell, “Fully Convolutional Networks for Semantic Segmentation”, in *Proceedings of the IEEE Conference on Computer Vision and Pattern Recognition*, 2015, pp. 3431–3440 (cit. on p. 9).

- [15] M. Turan, Y. Almalioglu, H. Araujo, E. Konukoglu, and M. Sitti, “Deep EndoVO: A recurrent convolutional neural network (RCNN) based visual odometry approach for endoscopic capsule robots”, *Neurocomputing*, vol. 275, pp. 1861–1870, Jan. 2018 (cit. on p. 10).
- [16] T. Ping-Sing and M. Shah, “Shape from shading using linear approximation”, *Image and Vision Computing*, vol. 12, no. 8, pp. 487–498, Oct. 1994 (cit. on p. 10).
- [17] K. Pogorelov, P. T. Schmidt, M. Riegler, P. Halvorsen, K. R. Randel, C. Griwodz, S. L. Eskeland, T. de Lange, D. Johansen, C. Spampinato, D.-T. Dang-Nguyen, and M. Lux, “KVASIR: A Multi-Class Image Dataset for Computer Aided Gastrointestinal Disease Detection”, in *Proceedings of the 8th ACM on Multimedia Systems Conference - MMSys’17*, 2017, pp. 164–169 (cit. on p. 12).
- [18] H. Borgli, V. Thambawita, P. H. Smedsrud, S. Hicks, D. Jha, S. L. Eskeland, K. R. Randel, K. Pogorelov, M. Lux, D. T. D. Nguyen, D. Johansen, C. Griwodz, H. K. Stensland, E. G. Ceja, P. T. Schmidt, H. L. Hammer, M. Riegler, P. Halvorsen, and T. de Lange, “Hyper-Kvasir: A Comprehensive Multi-Class Image and Video Dataset for Gastrointestinal Endoscopy”, Open Science Framework, Preprint, Dec. 2019 (cit. on p. 12).
- [19] G. Wallace, “The JPEG still picture compression standard”, *IEEE Transactions on Consumer Electronics*, vol. 38, no. 1, pp. xviii–xxxiv, Feb. 1992 (cit. on p. 12).